View metadata, citation and similar papers at core.ac.uk
brought to you by CORE
provided by Digital.CSIC

Hot spot analysis in integrated circuit substrates by laser mirage effect

X. Perpiñà,[1,a)] X. Jordà,[1] M. Vellvehi,[1] and J. Altet[2]
[1]Centre Nacional de Microelectrònica IMB-CNM (CSIC), Campus UAB, 08193 Bellaterra (Barcelona), Spain
[2]Departament d'Enginyeria Electrònica, Universitat Politècnica de Catalunya, Barcelona 08034, Spain

(Received 25 January 2011; accepted 31 March 2011; published online 22 April 2011)

This work shows an analytical and experimental technique for characterizing radial heat flow present in integrated circuits (ICs) when power is dissipated by integrated devices. The analytical model comes from the resolution of the Fermat equation for the trajectory of rays and supposing a spherical heat source dissipating a time-periodic power. An application example is presented; hence demonstrating how hot spots and heat transfer phenomena in the IC substrate can be characterized. The developed method may become a practical alternative to usual off-chip techniques for inspecting hot spots in ICs and to experimentally characterize heat flow in the semiconductor substrate. © *2011 American Institute of Physics*. [doi:10.1063/1.3581038]

Thermal sensing is a common practice in integrated circuits (ICs) when failure analysis,[1] system debugging,[2] or evaluation of their fabrication process dispersion[3] are performed. In this scenario, optically-based techniques have been widely used to thermally characterize ICs,[4,5] which have been mainly focused on hot spots detection.[6] Most of them access to the die by its top (front-side techniques) or back-side surfaces. Moreover, scaling and manufacturing tendencies increase both the number of metal layers[7] and the depth of passivation layers, stack different semiconductor dies in three-dimensional (3D) packed designs[8] or introduce the use of advanced cooling and heat spreading strategies.[9] Altogether raises the challenges that should be overcome when classical temperature measurement approaches are used[10] to perform an accurate thermal characterization.

This work proposes to characterize and locate hot spots (i.e., devices or structural defects) by sensing their thermal gradient inside the IC substrate by means of a laser beam probe, which longitudinally traverses the die (lateral access) as Fig. 1 shows. The hot spot detection is based on the Mirage effect:[11] The induced thermal gradient $[\vec{\nabla}T(r,t)]$ provokes a refractive index gradient $[\vec{\nabla}n(r,t)]$ within the IC substrate as[12]

$$\vec{\nabla}n(r,t) = \frac{\partial n}{\partial T}\vec{\nabla}T(r,t), \tag{1}$$

where $\partial n/\partial T$ is the so-called thermo-optical coefficient. Consequently, the beam trajectory is deflected toward the hot spot location in the plane defined by the heat source location $(x_0, 0, z_0)$ and the laser beam impinging point (X_0, Y_0, L) (Ref. 13) (see Fig. 1), according to the paraxial ray trace equation (small trajectory deviations)[13,14] inferred from Fermat's principle

$$\frac{d}{dz}(n\vec{\phi}_z) = \vec{\nabla}_{\perp}n(r,t), \tag{2}$$

where $\vec{\nabla}_{\perp}n(r,t)$ refers to the refractive gradient components corresponding to the directions perpendicular (x and y) to the laser beam propagation (z) (see Fig. 1) and $\vec{\phi}_z$ is the trajectory angular deflection experienced by the laser probe. Once the laser probe has totally traversed the IC substrate, its trajectory has experienced a total deflection $\vec{\Delta}_z$, described as

$$\vec{\Delta}_z = \int_0^L dz\vec{\phi}_z. \tag{3}$$

Eventually, $\vec{\Delta}_z$ is sensed by means of a deflection sensing system,[15] which directly determines its x- and y-Cartesian components (referred as horizontal and vertical) $\Delta_{z,h}$ and $\Delta_{z,v}$, respectively. This effect has been already exploited for materials local thermal properties determination[16,17] and for depth-resolved electrothermal characterization of power devices below the microsecond range.[11] Reference 11 reported that such kind of measurements are limited by the substrate doping level (e.g., $<10^{19}$ cm^{-3} for $L=2$ mm) and the upper metallizations presence: the chip substrate must be transparent to the laser beam and reflections on the top metallization may be avoided.

In this work, the procedure to perform the IC active thermal characterization consists in scanning the die perimeter with the laser beam at a given inspection depth Y_0 (lat-

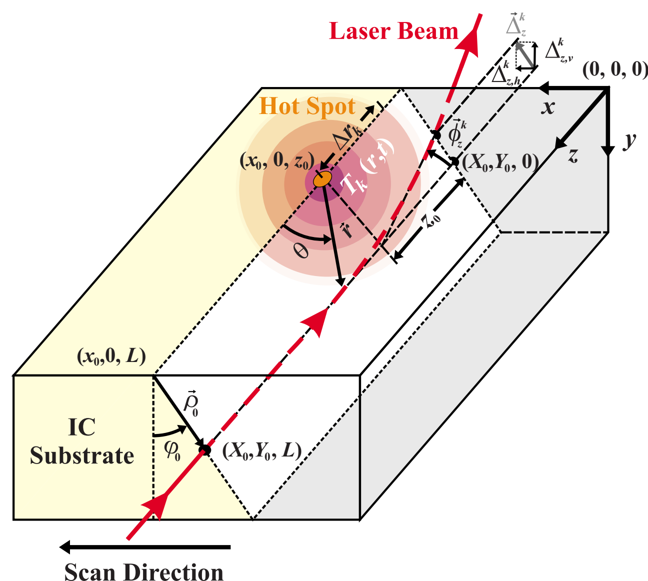

FIG. 1. (Color online) IC with a hot spot whose perimeter is scanned with a laser beam probe. All geometrical variables and magnitudes are also presented.

[a)]Electronic mail: xavier.perpinya@imb-cnm.csic.es.

Downloaded 08 Jun 2011 to 158.109.7.122. Redistribution subject to AIP license or copyright; see http://apl.aip.org/about/rights_and_permissions

eral access). This approach provides a faster thermal characterization of ICs in comparison to other optical punctual techniques,[4,9] being a complementary method when front-side or back-side approaches are not applicable. Besides, the limitations reported in Ref. 11 are not a problematic issue: the doping level in the IC substrates is low ($<10^{16}$ cm^{-3}) and measurements may be performed at Y_0 deeper than the beam diameter avoiding metallization reflections. To show its feasibility in this scenario, an analytical model about this approach is first derived when small devices or structural defects dissipate power (hot spots). After this, measurements on an IC based on complementary metal-oxide-semiconductor technology are compared to the derived model.

Figure 1 also outlines the thermal behavior within the IC substrate when integrated devices or structural defects dissipate a power waveform described by a periodic function of frequency f (usual working conditions in digital circuits). In this situation, the thermal field $T(r,t)$ generated by the hot spot within the IC substrate can be expanded in a Fourier series,[18] with harmonic components $T_k(r,t)$. By selecting a suitable value for f, it is possible to consider $T_k(r,t)$ confined within the silicon substrate following a radial distribution with spherical symmetry (punctual heat source approximation),[18] as Fig. 1 depicts in spherical coordinates (r,φ_0,θ). Therefore, $\vec{\nabla}T(r,t)$ has the following kth harmonic component $\vec{\nabla}T_k(r,t)$ outside the power generation region[18]

$$\vec{\nabla}T_k(r,t) = \mathrm{Re}[-C_k(1+r\xi_k)/r^2 \exp(-r\xi_k + i2\pi kft)]\hat{u}_r, \tag{4}$$

where C_k refers to the Fourier constant, r corresponds to the distance from the heat source, and $\hat{u}_r$ represents the unit vector corresponding to the radial direction from the heat source (see Fig. 1). ξ_k is a complex constant which depends on f, k, and the material thermal diffusivity D_α as $\xi_k=(1+i)\sqrt{\pi kf/D_\alpha}$. To determine the penetration depth of the thermal energy into the IC substrate, a characteristic depth d_k is defined as $d_k=\sqrt{D_\alpha/(\pi kf)}$, which corresponds to the thermal diffusion length.[5] Consequently, $T_k(r,t)$ and $\vec{\nabla}T_k(r,t)$ are confined within the substrate in a hemisphere of radius Δr_k, which can be expressed as a multiple of d_k,[18] i.e., $\Delta r_k=md_k$ (see Fig. 1). Moreover, by selecting a suitable value of k or f, the radius of the thermal disturbance provoked by the kth harmonic of the dissipated power can be externally controlled with high accuracy. Due to the linear dependency expressed in (1) and (2), $\vec{\phi}_z$ and $\vec{\Delta}_z$ can be as well decomposed into Fourier harmonics, referred as $\vec{\phi}_z^k$ and $\vec{\Delta}_z^k$, respectively. The amplitude and phase of the Cartesian components of $\vec{\Delta}_z^k$ ($\Delta_{z,h}^k$ and $\Delta_{z,v}^k$, see Fig. 1) can be directly measured connecting the deflection sensing system to a lock-in amplifier, providing the signals $V_{out,h}^k$ and $V_{out,v}^k$.

In order to obtain a final expression for $V_{out,h}^k$ and $V_{out,v}^k$ as a function of the hot spot location, the scanning direction (see Fig. 1), and the monitored $\vec{\nabla}T_k(r,t)$; $\vec{\phi}_z^k$ is first derived by solving Eq. (2) in cylindrical coordinates (ρ_0,φ_0,z) and considering n weakly dependent on $T(r,t)$ (i.e., $n\approx n_0$):[12]

$$\vec{\phi}_z^k(\rho_0,\varphi_0) = \frac{\rho_0}{n_0}\frac{\partial n}{\partial T}[-\sin(\varphi_0)\hat{u}_x + \cos(\varphi_0)\hat{u}_y]\mathrm{Re}[-C_k \exp(i2\pi kft)I(\varphi_0,k)], \tag{5}$$

where $\rho_0=\sqrt{(X_0-x_0)^2+Y_0^2}$, $\varphi_0=\tan^{-1}[(X_0-x_0)/Y_0]$, n_0 is the refractive index of the substrate at ambient temperature, and X_0 (Y_0) corresponds to the lateral (vertical) coordinate of the beam impinging point (see Fig. 1). $I(\varphi_0,k)$ is the sum of $\vec{\nabla}T_k(r,t)$ found along the beam trajectory, and writes as

$$I(\varphi_0,k) = \int_{r_i}^{r_f} dr \frac{(1+\xi_k r)\exp(-\xi_k r)}{r^2\sqrt{r^2-[Y_0/\cos(\varphi_0)]^2}}, \tag{6}$$

where r_i (r_f) is the lower (upper) integration limit. Equation (6) can be solved analytically assuming: First, the radial coordinate ρ_0 of the laser impinging point should be bigger than d_k (i.e., $\rho_0>d_k$), allowing: $\exp(-\xi_k r)\approx(1-\xi_k r+(\xi_k r)^2/2)$. Second, $\vec{\nabla}T_k(r,t)$ is negligible outside the range Δr_k, i.e., $\vec{\nabla}T_k(r,t)\approx 0$ in the limiting boundary of the hemisphere with radius Δr_k. With these assumptions $r_i=\rho_0$ and $r_f=\Delta r_k$ and the amplitude of $I(\varphi_0,k)$ ($|I(\varphi_0,k)|$) is

$$|I(\varphi_0,k)| \approx 2\left[\frac{[\cos^2(\varphi_0)-Y_0^2/\Delta r_k^2]\cos^2(\varphi_0)}{Y_0^4} + \frac{1}{4d_k^4} \times \ln^2\left(\frac{\cos(\varphi_0)-\sqrt{\cos^2(\varphi_0)-Y_0^2/\Delta r_k^2}}{\cos(\varphi_0)+\sqrt{\cos^2(\phi_0)-Y_0^2/\Delta r_k^2}}\right)\right]^{1/2}. \tag{7}$$

When measurements are performed, the previous assumptions are valid by selecting suitable values for f, k, and Y_0 (i.e., $Y_0>d_k$ and $\Delta r_k>Y_0$). Finally, the expressions for the amplitude of $V_{out,h}^k$ and $V_{out,v}^k$ [$|V_{out,h}^k(\rho_0,\varphi_0)|$ and $|V_{out,v}^k(\rho_0,\varphi_0)|$, respectively] are inferred by assuming small deflections (paraxial approximation), which allows to rewrite Eq. (3) as $\vec{\Delta}_z^k\approx\vec{\phi}_z^k z_0$. Knowing that $|V_{out,h}^k(\rho_0,\varphi_0)|$ and $|V_{out,v}^k(\rho_0,\varphi_0)|$ are proportional to $\Delta_{z,h}^k$ and $\Delta_{z,v}^k$, these expressions are derived

$$|V_{out,h}^k(\rho_0,\varphi_0)| = \gamma_h\frac{z_0}{n_0}\frac{\partial n}{\partial T}C_k\rho_0\sin(\varphi_0)|I(\varphi_0,k)|, \tag{8}$$

$$|V_{out,v}^k(\rho_0,\varphi_0)| = -\gamma_v\frac{z_0}{n_0}\frac{\partial n}{\partial T}C_k\rho_0\cos(\varphi_0)|I(\varphi_0,k)|, \tag{9}$$

where γ_h and γ_v are the proportionality factors among the output signals and the total deflection Cartesian components.[11]

Analyzing in more detail the product $\rho_0\cdot|I(\varphi_0,k)|$ as a function of φ_0, it can be observed that $\rho_0\cdot|I(\varphi_0,k)|$ corresponds to an even symmetric decreasing function of φ_0 with a maximum value for $\varphi_0=0$ (beneath the device acting as hot spot). Notice that $|V_{out,h}^k(\varphi_0)|$ and $|V_{out,v}^k(\varphi_0)|$ are obtained by multiplying Eqs. (8) and (9) with $\sin(\varphi_0)$ or $\cos(\varphi_0)$, respectively. Therefore, the hot spot will be located when $|V_{out,h}^k(\varphi_0)|$ and $|V_{out,v}^k(\varphi_0)|$ will present minimum and maximum values at the same time.

This approach has been verified with a specific IC ($3075\times2350\times500$ μm^3), which has been developed to measure the thermal coupling generated by the transistors

Downloaded 08 Jun 2011 to 158.109.7.122. Redistribution subject to AIP license or copyright; see http://apl.aip.org/about/rights_and_permissions

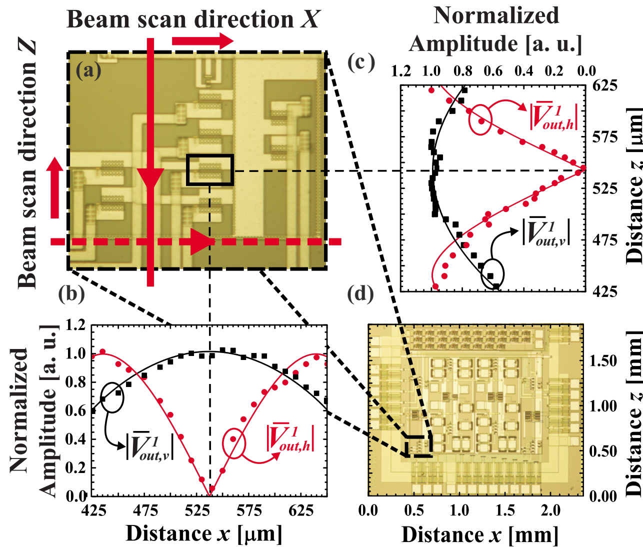

FIG. 2. (Color online) (a) Location of the device behaving as a hot spot. (b) and (c) shows the amplitude of the vertical and horizontal beam deflection components for $k=1$ as a function of the IC layout x- and z-coordinate, respectively. (d) IC top view photograph.

acting as hot spots [partially shown in Fig. 2(d)]. In this IC, there are 16 dissipating devices consisting in metal-oxide-semiconductor field effect transistors with a channel size $20\times 1.2\ \mu m^2$ and connected in diode configuration, i.e., source tied to ground and gate connected to the drain. In addition, each gate is directly accessible through a pin, allowing the individual activation of each device. The square in Fig. 2(a) indicates the location of the transistor activated to generate the hot spot. In the experiments, this transistor has been stimulated in such a way that the power dissipated was periodic (5 V voltage square waveform); with a frequency of 2120 Hz and amplitude of 25 mW. In this work, only the amplitude of the first harmonic ($k=1$) of $V_{out,v}$ and $V_{out,h}$ has been considered (i.e., $|V^1_{out,v}|$ and $|V^1_{out,h}|$), as indicated in Fig. 2(b). All measurements have been performed at the inspection depth $Y_0=180\ \mu m$, which is deeper than d_1 (characteristic depth when $k=1$, 116 μm). In this way, the approximations performed to derive Eqs. (8) and (9) are fulfilled. Moreover, as Eq. (4) indicates, $\vec{\nabla} T_1(r,t)$ is strongly attenuated at the selected Y_0, expecting to detect low signal levels for $|V^1_{out,v}|$ and $|V^1_{out,h}|$. As a result, this will provide an idea of the approach's sensitivity, since these measurement conditions are not the optimum ones.

Figures 2(b) and 2(c) plot the experimental normalized amplitudes of $V_{out,v}$ and $V_{out,h}$ ($|\bar{V}^1_{out,v}|$ and $|\bar{V}^1_{out,h}|$, respectively) after a perimeter scan along the directions x and z as defined in Fig. 1, together with the fittings of Eqs. (8) and (9) for each situation. When the lateral scanning is performed along the z-direction (laser propagates through x-direction), Eqs. (8) and (9) and the definition of φ_0 should be modified as follows: z_0 by x_0, $\hat{u}_x$ by $\hat{u}_z$, and X_0 by Z_0. The fitting parameters have been the hot spot lateral positions (i.e., x_0 and z_0) and Δr_1. In this case, $x_0=537\pm 1\ \mu m$, $z_0=542\pm 1\ \mu m$, and $\Delta r_1=233\pm 3\ \mu m$ have been obtained. The error has been computed accounting for both the lateral resolution fixed by the positioning stage accuracy (1 μm) and the model sensitivity. From Fig. 2, a high agreement is observed between experiment and the predictions of Eqs. (8) and (9).

When the IC perimeter is inspected (two lateral sides along the x and z axis), the device acting as a hot spot is located at the point where $|\bar{V}^1_{out,v}|$ is maximum and $|\bar{V}^1_{out,h}|$ nulls [see Figs. 2(b) and 2(c)], as previously indicated. Notice that not only this technique has been capable to detect the hot spot when the impinging point of the laser is at a deeper position from the die surface, but also permits to perform characterization of the thermal coupling and the heat transfer within the substrate avoiding the beam reflections on the top metallization. For instance, Δr_1 can be derived by fitting Eqs. (8) and (9) to the measured $|\bar{V}^1_{out,v}|$ and $|\bar{V}^1_{out,h}|$ values. From the reported measurements, $\Delta r_1=233\pm 3\ \mu m$, which implies a factor $m=2.008$.

In summary, this work proposes an alternative approach to ICs active thermal characterization when for instance, 3D stacked ICs or top metallization limits their characterization by the existing techniques. It accesses to the die laterally, allowing us to scan its perimeter.

This work has been partially supported by the Consejo Superior de Investigaciones Científicas (CSIC) (under contract "Junta para la Ampliación de Estudios," JAEDoc No. E-08–2008–0637732) and the Spanish Ministry of Science and Innovation (research programs THERMOS TEC2008-05577, RUE CSD2009-00046, TERASYSTEMS TEC2008-01856, and Ramón y Cajal RYC-2010-07434).

[1]M. Pedram and S. Nazarian, Proc. IEEE **94**, 1487 (2006).
[2]S. Mattisson, H. Hagberg, and P. Andreani, IEEE J. Solid-State Circuits **43**, 486 (2008).
[3]J. Jaffari and M. Anis, IEEE Trans. Comput.-Aided Des. **27**, 1027 (2008).
[4]S. Y. Suck, G. Tessier, N. Warnasooriya, A. Babuty, and Y. De Wilde, Appl. Phys. Lett. **96**, 121108 (2010).
[5]L. Aigouy, G. Tessier, M. Mortier, and B. Charlot, Appl. Phys. Lett. **87**, 184105 (2005).
[6]J. Altet, M. A. Salhi, S. Dilhaire, A. Syal, and A. Ivanov, Electron. Lett. **39**, 1440 (2003).
[7]A. Nieuwoudt, J. Kawa, and Y. Massoud, IEEE Trans. Very Large Scale Integr. (VLSI) Syst. **18**, 378 (2010).
[8]K. Nomura, T. Aoki, K. Nakamura, T. Kamiya, T. Nakanishi, T. Hasegawa, M. Kimura, T. Kawase, M. Hirano, and H. Hosono, Appl. Phys. Lett. **96**, 263509 (2010).
[9]S. Ghosh, I. Calizo, D. Teweldebrhan, E. P. Pokatilov, D. L. Nika, A. A. Balandin, W. Bao, F. Miao, and C. N. Lau, Appl. Phys. Lett. **92**, 151911 (2008).
[10]J. Altet, W. Claeys, S. Dilhaire, and A. Rubio, Proc. IEEE **94**, 1519 (2006).
[11]X. Perpiñà, *Power Devices Electrothermal Characterization by Optical Techniques: An Experimental Approach to Analyze Internal Electrothermal Phenomena at Device Level* (VDM Verlag Dr. Mueller e.K, Saabrücken, 2008).
[12]A. N. Magunov, Opt. Spectrosc. **73**, 205 (1992).
[13]M. Born and E. Wolf, *Principles of Optics*, 6th ed. (Pergamon, Exeter, 1989).
[14]L. W. Casperson, Appl. Opt. **12**, 2434 (1973).
[15]X. Perpiñà, X. Jordà, M. Vellvehi, J. Millán, and N. Mestres, Rev. Sci. Instrum. **76**, 025106 (2005).
[16]A. C. Boccara, D. Fournier, and J. Badoz, Appl. Phys. Lett. **36**, 130 (1980).
[17]J. D. Spear and R. E. Russo, J. Appl. Phys. **70**, 580 (1991).
[18]H. S. Carslaw and J. C. Jaegger, *Conduction of Heat in Solids*, 2nd ed. (Clarendon, Oxford, 1986).
[19]X. Perpiñà, X. Jordà, M. Vellvehi, J. Altet, and N. Mestres, J. Phys. D: Appl. Phys. **41**, 155508 (2008).

Downloaded 08 Jun 2011 to 158.109.7.122. Redistribution subject to AIP license or copyright; see http://apl.aip.org/about/rights_and_permissions